

Effects of Couple Stresses on Stress Distributions in a Ring Test Specimen

By

Shoichi KOBAYASHI* and Takuo FUKUI**

(Received June 30, 1971)

The ring test is often used to estimate the tensile strength of rock-like materials. The results of the test, however, are not well interpreted by the classical theory of elasticity. The present paper, with the intention of a better interpretation of the results, discusses the effects of couple stresses on the stress distributions in a ring test specimen. An analytic solution was obtained by the Fourier-Bessel expansion method. Results show that the effects of couple stresses are remarkable. As the intrinsic internal length of material increases, the stresses rapidly decrease and become more uniform. The Poisson's ratio decreases, and more uniform stresses are developed. However, its effects are secondary in comparison with the intrinsic internal length of material.

1. Introduction

The ring test is often used to estimate the tensile strength of rock-like materials in preference to the Brazilian test, because the stress field in the former is simpler than in the latter.¹⁾ The theoretical foundation of the ring test has been given in several papers.²⁻⁴⁾ Unfortunately, as was reported by Addinal and Hackett,¹⁾ Koyanagi *et al.*⁵⁾ and further discussed by Hudson,⁶⁾ all the test results indicated widely different tensile strengths. The main reason for the variation of the tensile strength was reported to be that the calculated stress based on the classical theory of elasticity is not the 'real' stress for rock-like materials.^{1,6)}

As is well known, the classical theory of elasticity assumes the homogeneity of the constituent materials to an infinitesimal element of volume, that is, mass density is continuous and remains constant if any volume element is continuously shrunk to zero. This continuum approximation is violated for many materials composed of several distinct constituent materials, for example,

* Department of Civil Engineering

** Graduate Student

for polycrystalline mixtures such as rocks, and for composite materials. The classical theory of elasticity is successfully applied to the analysis of stress wherever the overall dimension of the concerned problem is larger than the average dimension of the intrinsic discontinuities in the material, for example, average grain size or inter-grain distance. However, as the ratio of the overall dimension of the problem to the average internal length of material approaches unity, the classical theory of elasticity is expected to fail. In such a case, a more precise theory which reflects the effects of the constituent materials must be sought for.

The couple stress theory^{7,8)} or the micropolar theory⁹⁾ may find applications in a wide variety of situations from crystal lattices to rocks or composite materials. As was discussed by Eringen⁹⁾ and Cowin,¹⁰⁾ the couple stress theory is an extreme of the micropolar theory and the classical theory is another extreme. In other words, the real response of materials falls between that predicted by the couple stress theory and that predicted by the classical theory.

The present paper discusses the effects of the average internal length of material on the stress distributions in a ring specimen subjected to diametral compression. Similar effects in the Brazilian test specimen were discussed in a companion paper.¹¹⁾ These results may provide some explanation for the variation of the ring tensile strength.

2. Description of the Problem

A ring specimen of external radius a and internal radius b was loaded by a radial load applied over the opposite arcs of its outer surface as shown in Fig. 1. The specimen was assumed to obey the couple stress theory of elasticity and to be in a state of plane strain.

According to Mindlin,⁷⁾ the governing equations of the couple stress theory of elasticity are expressed in the general coordinates x^α ($\alpha=1, 2$) by the two stress functions ϕ and ψ as follows:

$$\Delta^4 \phi = 0 \quad (2.1)$$

$$(1 - l^2 \nabla^2) \nabla^2 \psi = 0 \quad (2.2)$$

$$(1 - l^2 \nabla^2) \phi|_\alpha = -2(1 - \nu) l^2 \varepsilon_{3\alpha\beta} g^{\beta\gamma} \nabla^2 \phi|_\gamma \quad (2.3)$$

where $\nabla^2 = \frac{1}{\sqrt{g}} \frac{\partial}{\partial x^\alpha} \left(\sqrt{g} g^{\alpha\beta} \frac{\partial}{\partial x^\beta} \right)$, $\nabla^4 = \nabla^2 \cdot \nabla^2$, $g = \det |g_{\alpha\beta}|$

$g_{\alpha\beta}$, $\varepsilon_{3\alpha\beta}$, ν and l are the fundamental metric tensor, the permutation tensor, the Poisson's ratio, and the internal length of material implying the bending

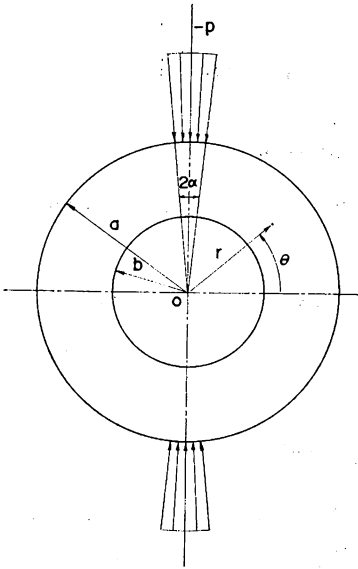


Fig. 1. Schematic diagram of the ring test and the coordinate system.

rigidity of a micro-element, respectively, and $\psi|_{\alpha}$ implies the covariant derivative of ψ by x^{α} .

Stresses are expressed by the stress functions :

$$\tau^{\alpha\beta} = \epsilon^{3\alpha\gamma} \epsilon^{3\beta\delta} \phi|_{\gamma\delta} + \epsilon^{3\gamma\alpha} \psi|_{\gamma\beta} \tag{2.4}$$

$$\mu_{3\alpha} = \psi|_{\alpha} \tag{2.5}$$

where $\tau^{\alpha\beta}$ and $\mu_{3\alpha}$ are the Cauchy stress and the couple stress, respectively.

When $l=0$, these expressions are reduced to those of the classical theory of elasticity.

The solution of the problem of the couple stress theory of elasticity is thus obtained by solving the governing equations (2.1) to (2.3) with appropriate boundary conditions.

The boundary conditions of the present problem are expressed in the polar coordinates (r, θ) as follows :

$$\sigma_r(a, \theta) = p(\theta), \quad \tau_{r\theta}(a, \theta) = 0, \quad m_r(a, \theta) = 0 \tag{2.6}$$

$$\sigma_r(b, \theta) = 0, \quad \tau_{r\theta}(b, \theta) = 0, \quad m_r(b, \theta) = 0 \tag{2.7}$$

where notations for stresses are redefined such that σ_r , $\tau_{r\theta}$, and m_r express the components of the normal stress, the shear stress, and the couple stress, respectively.

The surface load of the present problem is expressed in the Fourier cosine series as

$$\left. \begin{aligned} p(\theta) &= \frac{1}{2}f_0 + \sum_{n=1}^{\infty} f_n \cos n\theta \\ f_n &= \frac{2}{\pi} \int_0^{\pi} p(\theta) \cos n\theta d\theta \end{aligned} \right\} \quad (2.8)$$

3. Analytical Solution

The analytical solutions of Eqs. (2.1) and (2.2) of the present problem are expressed

$$\phi = A_0 l n r + B_0 r^2 + \sum_{n=2,4,\dots}^{\infty} (A_n r^{n+2} + B_n r^{-n} + C_n r^{-n+2} + D_n r^{-n}) \cos n\theta \quad (3.1)$$

$$\begin{aligned} \psi &= a_0 l n r + \sum_{n=2,4,\dots}^{\infty} (a_n r^n + b_n r^{-n}) \sin n\theta \\ &+ \sum_{n=2,4,\dots}^{\infty} \left\{ d_n I_n\left(\frac{r}{l}\right) + e_n K_n\left(\frac{r}{l}\right) \right\} \sin n\theta \end{aligned} \quad (3.2)$$

where $I_n\left(\frac{r}{l}\right)$ and $K_n\left(\frac{r}{l}\right)$ are the modified Bessel functions of the first and the second kind, respectively, and $A_0, B_0, A_n, B_n, \dots, a_0, a_n, b_n, \dots$ are constants to be determined.

Substituting Eqs. (3.1) and (3.2) into Eq. (2.3), the following relations are obtained

$$\left. \begin{aligned} a_0 &= 0 \\ a_n &= 8(1-\nu)(n+1)l^2 A_n \\ b_n &= 8(1-\nu)(n-1)l^2 C_n \end{aligned} \right\} \quad (3.3)$$

Stresses are obtained by substituting Eqs. (3.1) and (3.2) into Eqs. (2.4) and (2.5) as follows:

$$\begin{aligned} \sigma_r &= r^{-1}\phi_{,r} + r^{-2}\phi_{,\theta\theta} - r^{-1}\psi_{,r\theta} + r^{-2}\psi_{,\theta} \\ &= r^{-2}A_0 + 2B_0 \\ &+ \sum_{n=2,4,\dots}^{\infty} \{(-n+2)(n+1)r^n A_n - n(n-1)r^{n-2}B_n \\ &\quad - (n+2)(n-1)r^{-n}C_n - n(n+1)r^{-n-2}D_n\} \cos n\theta \\ &+ \sum_{n=2,4,\dots}^{\infty} \{-n(n-1)r^{n-2}a_n + n(n+1)r^{-n-2}b_n\} \cos n\theta \\ &+ \sum_{n=2,4,\dots}^{\infty} \{n(r^{-2}I_n - r^{-1}I_n')d_n + n(r^{-2}K_n - r^{-1}K_n')e_n\} \cos n\theta \end{aligned} \quad (3.4)$$

$$\begin{aligned} \sigma_\theta &= \phi_{,rr} + r^{-1}\psi_{,\theta\theta} - r^{-2}\psi_{,\theta} \\ &= -r^{-2}A_0 + 2B_0 \\ &+ \sum_{n=2,4,\dots}^{\infty} \{(n+2)(n+1)r^n A_n + n(n-1)r^{n-2}B_n \\ &\quad + (n-2)(n-1)r^{-n}C_n + n(n+1)r^{-n-2}D_n\} \cos n\theta \end{aligned}$$

$$\begin{aligned}
& + \sum_{n=2,4,\dots}^{\infty} \{n(n-1)r^{n-2}a_n - n(n+1)r^{-n-2}b_n\} \cos n\theta \\
& + \sum_{n=2,4,\dots}^{\infty} \{n(-r^{-2}I_n + r^{-1}I_n')d_n + n(-r^{-2}K_n + r^{-1}K_n')e_n\} \cos n\theta \quad (3.5)
\end{aligned}$$

$$\begin{aligned}
\tau_{r\theta} &= -r^{-1}\phi_{,r\theta} + r^{-2}\phi_{,\theta} - r^{-1}\psi_{,r} - r^{-2}\psi_{,\theta\theta} \\
&= -r^{-2}a_0 \\
& + \sum_{n=2,4,\dots}^{\infty} \{n(n+1)r^n A_n + n(n-1)r^{n-2}B_n \\
& \quad - n(n-1)r^{-n}C_n - n(n+1)r^{-n-2}D_n\} \sin n\theta \\
& + \sum_{n=2,4,\dots}^{\infty} \{n(n-1)r^{n-2}a_n + n(n+1)r^{-n-2}b_n\} \sin n\theta \\
& + \sum_{n=2,4,\dots}^{\infty} \{(n^2r^{-2}I_n - r^{-1}I_n')d_n + (n^2r^{-2}K_n - r^{-1}K_n')e_n\} \sin n\theta \quad (3.6)
\end{aligned}$$

$$\begin{aligned}
\tau_{\theta r} &= -r^{-1}\phi_{,r\theta} + r^{-2}\phi_{,\theta} + \psi_{,rr} \\
&= -r^{-2}a_0 \\
& + \sum_{n=2,4,\dots}^{\infty} \{n(n+1)r^n A_n + n(n-1)r^{n-2}B_n \\
& \quad - n(n-1)r^{-n}C_n - n(n+1)r^{-n-2}D_n\} \sin n\theta \\
& + \sum_{n=2,4,\dots}^{\infty} \{n(n-1)r^{n-2}a_n + n(n+1)r^{-n-2}b_n\} \sin n\theta \\
& + \sum_{n=2,4,\dots}^{\infty} \{I_n''d_n + K_n''e_n\} \sin n\theta \quad (3.7)
\end{aligned}$$

$$\begin{aligned}
m_r &= \psi_{,r} \\
&= r^{-1}a_0 \\
& + \sum_{n=2,4,\dots}^{\infty} \{nr^{n-1}a_n - nr^{-n+1}b_n\} \sin n\theta \\
& + \sum_{n=2,4,\dots}^{\infty} \{I_n'd_n + K_n'e_n\} \sin n\theta \quad (3.8)
\end{aligned}$$

$$\begin{aligned}
m_\theta &= r^{-1}\psi_{,\theta} \\
&= \sum_{n=2,4,\dots}^{\infty} n\{r^{n-1}a_n + r^{-n-1}b_n\} \cos n\theta \\
& + \sum_{n=2,4,\dots}^{\infty} nr^{-1}\{I_n d_n + K_n e_n\} \cos n\theta \quad (3.9)
\end{aligned}$$

where I_n' and K_n' represent derivatives of $I_n\left(\frac{r}{l}\right)$ and $K_n\left(\frac{r}{l}\right)$ by $\frac{r}{l}$, respectively.

Substitution of Eqs. (3.4), (3.6) and (3.8) into the boundary conditions (2.6) and (2.7) furnishes the following system of linear equations of unknown coefficients:

$$\begin{aligned}
a^{-2}A_0+2B_0 &= \frac{1}{2}f_0 \\
(-n+2)(n+1)a^nA_n-n(n-1)a^{n-2}B_n-(n+2)(n-1)a^{-n}C_n-n(n+1)a^{-n-2}D_n \\
&\quad -n(n-1)a^{n-2}a_n+n(n+1)a^{-n-2}b_n \\
&\quad +n(a^{-2}I_n-a^{-1}I_n')d_n+n(a^{-2}K_n-a^{-1}K_n')e_n \\
&=f_n
\end{aligned} \tag{3.11}$$

$$\begin{aligned}
n(n+1)a^nA_n+n(n-1)a^{n-2}B_n-n(n-1)a^{-n}C_n-n(n+1)a^{-n-2}D_n \\
&\quad +n(n-1)a^{n-2}a_n+n(n+1)a^{-n-2}b_n \\
&\quad +(n^2a^{-2}I_n-a^{-1}I_n')d_n+(n^2a^{-2}K_n-a^{-1}K_n')e_n \\
&=0
\end{aligned} \tag{3.12}$$

$$na^{n-1}a_n-na^{n-1}b_n+I_n'd_n+K_n'e_n=0 \tag{3.13}$$

$$b^{-2}A_0+2B_0=0 \tag{3.14}$$

$$\begin{aligned}
(-n+2)(n+1)b^nA_n-n(n-1)b^{n-2}B_n-(n+2)(n-1)b^{-n-1}C_n-n(n+1)b^{-n-2}D_n \\
&\quad -n(n-1)b^{n-2}a_n+n(n+1)b^{-n-2}b_n \\
&\quad +n(b^{-2}I_n-b^{-1}I_n')d_n+n(b^{-2}K_n-b^{-1}K_n')e_n \\
&=0
\end{aligned} \tag{3.15}$$

$$\begin{aligned}
n(n+1)b^nA_n+n(n-1)b^{n-2}B_n-n(n-1)b^{-n}C_n-n(n+1)b^{-n-2}D_n \\
&\quad +n(n-1)b^{n-2}a_n+n(n+1)b^{-n-2}b_n \\
&\quad +(n^2b^{-2}I_n-b^{-1}I_n')d_n+(n^2b^{-2}K_n-b^{-1}K_n')e_n \\
&=0
\end{aligned} \tag{3.16}$$

$$nb^{n-1}a_n-nb^{n-1}b_n+I_n'd_n+K_n'e_n=0 \tag{3.17}$$

The unknown coefficients are $8n+3$ and can be determined from the $6n+2$ equations of Eqs. (3.10) to (3.16) and the $2n+1$ equations of Eq. (3.3).

In the numerical computations, the higher terms of the equations are forced to truncate due to the limited capacity of the computer. In the present computation, the terms higher than $n=52$ and $n=32$ were truncated for $\frac{b}{a} \geq 0.5$ and 0.3 , respectively. The values of the modified Bessel functions were calculated by Miller's method.

4. Results and Discussion

The collected results of stresses on typical diametral sections are shown in Figs. 2 to 4. The results correspond to the case in which the surface load p is uniformly distributed over the opposite arcs $2\alpha a$, with $\alpha=2.5^\circ$. Stresses are also normalized by $P/\pi a$ ($P=2\alpha ap$), which is the tensile stress at the center of the specimen of the Brazilian test obtained by the classical theory

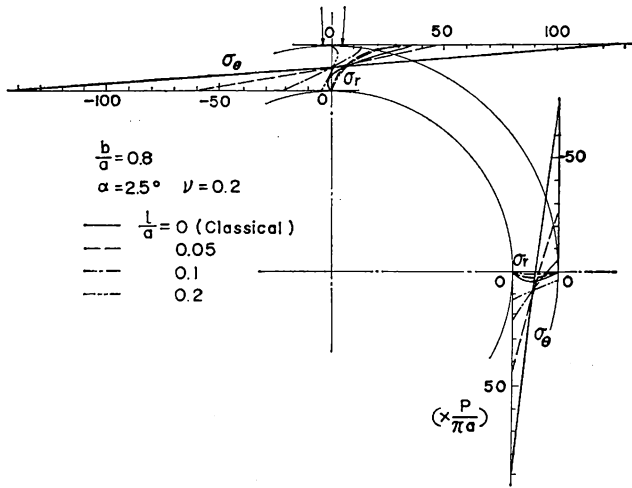


Fig. 2. Effects of the internal length of material l on the stress distributions when $\frac{b}{a}=0.8$ and $\nu=0.2$.

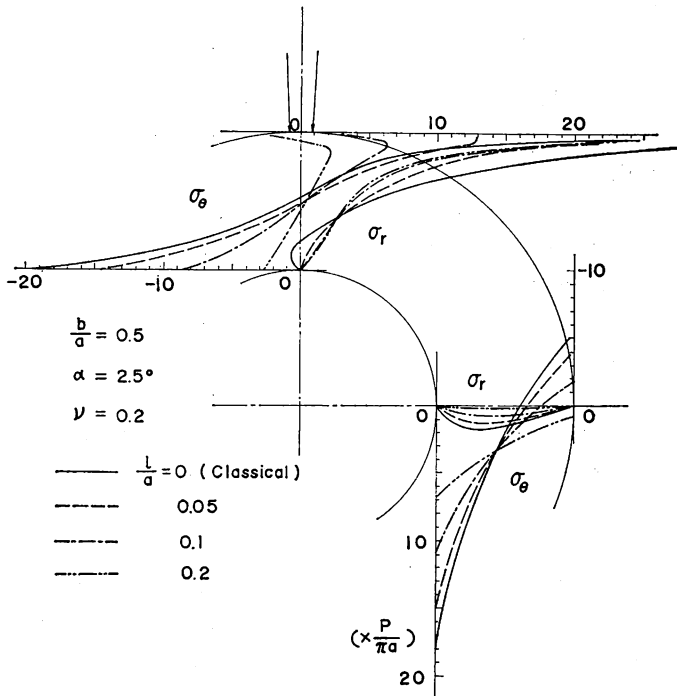


Fig. 3. Effects of the internal length of material l on the stress distributions when $\frac{b}{a}=0.5$ and $\nu=0.2$.

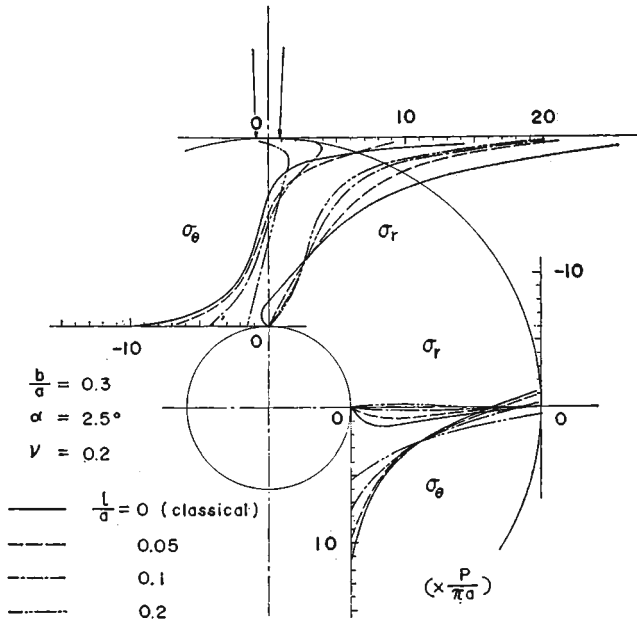


Fig. 4. Effects of the internal length of material l on the stress distributions when $\frac{b}{a}=0.3$ and $\nu=0.2$.

of elasticity. These figures indicate the remarkable influence of the internal length of material, l . As l increases, the stresses are strikingly reduced and become more uniform. Also, as the ratio of the inner radius to the outer increases, the stress distributions are more nearly approximated by those expected from the bending theory of bars. On the other hand, as the ratio decreases, the stress distributions are expected to become more and more uniform over the whole region of the specimen as anticipated from the Brazilian test results (except near the inner boundary).

Stresses at the inner edge on the diametral section in the loading direction are shown in Fig. 5 as a function of the ratio of the inner radius to the outer. Reduction of stress concentration with an increase of l is clearly demonstrated. However small the inner radius is, stresses at the edge of the hole do not reduce to those of the Brazilian test. As the internal length of material increases, the former gradually decreases toward the latter. However, it must be noted that the limiting condition, *i. e.* $b/a \rightarrow 0$, is meaningless in the couple stress theory, because the internal length of material should be smaller or at least on the same order of the diameter of the hole, otherwise the real 'signals' of stress concentration are lost amid the background 'noise' of the intrinsic discontinuities of materials. These results may help the interpretation of the

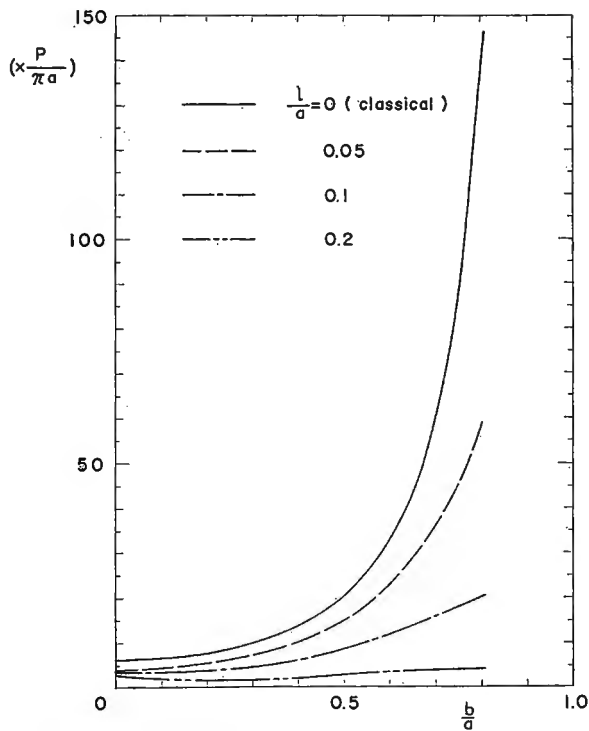


Fig. 5. Variations of stresses at the inner edge on the diametral section in the loading direction with the ratio of the inner radius to the outer.

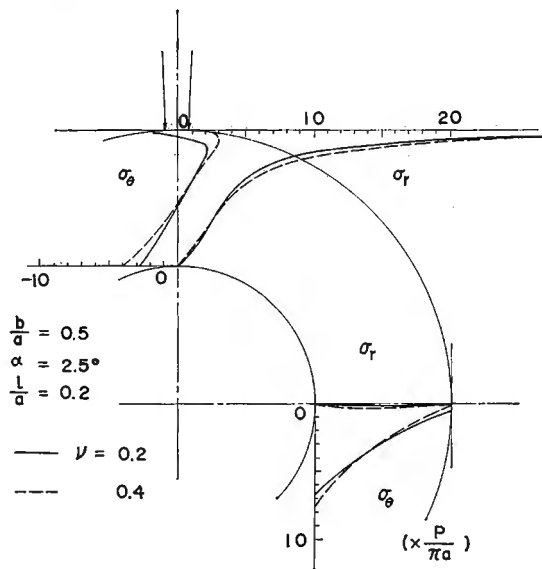


Fig. 6. Effects of the Poisson's ratio on the stress distributions.

variation of tensile strength by the ring test.

The influence of the Poisson's ratio on the stress distributions is shown in Fig. 6. As the Poisson's ratio decreases, more uniform stress distributions are developed. The effects, however, are not so predominant as those of the internal length of material.

5. Concluding Remarks

The analytical results indicate that couple stresses have remarkable effects on the stress distributions in the ring test specimen. The reduction of stress concentration with an increase of the internal length of material is striking. The fact may suggest the appropriate interpretation of the ring test results.

Acknowledgement

The numerical computations were performed on the FACOM 230-60 computer, at the Computation Center of Kyoto University.

References

- 1) Addinal E. and P. Hackett : Proc. 6th Rock Mech. Symp., Rolla, Missouri (1964).
- 2) Ripperger E. and N. Davids : Trans. Am. Soc. Civ. Engrs, **112**, pp. 619-627 (1947).
- 3) Jaeger J. C. and E. R. Hoskins : Brit. J. Appl. Phys., **17**, pp. 685-692 (1966).
- 4) Peterson R. E. : "STRESS CONCENTRATION DESIGN FACTORS", 3rd Ed., p. 135, John Wiley & Sons (1962).
- 5) Koyanagi W., S. Kobayashi, Y. Inoue and K. Yamamoto : Review of 21st General Meeting, The Cement Assoc. of Japan, pp. 127-130 (1968).
- 6) Hudson J. A. : Int. J. Rock Mech. Min. Sci., **6**, pp. 91-97 (1969).
- 7) Mindlin R. D. : Exp. Mech., **3**, pp. 1-7 (1963).
- 8) Mindlin R. D. and H. F. Tiersten : Archiv. Rat. Mech. Anal., **11**, pp. 415-448 (1962).
- 9) Eringen A. C. : Theory of Micropolar Elasticity, Chapt. 7 in "FRACTURE II", H. Liebowitz (Ed.), pp. 621-729, Academic Press (1968).
- 10) Cowin S. C. : ZAMP, **21**, pp. 494-497 (1970).
- 11) Niwa Y., S. Kobayashi and T. Fukui : Memo. Faculty of Eng., Kyoto Univ. **32**, pp. 118-127 (1971).